

Synthesis and Evaluation of 4-Bromo-1-(3-[¹⁸F]fluoropropyl)-2-nitroimidazole with a Low Energy LUMO Orbital Designed as Brain Hypoxia-Targeting Imaging Agent

Fumihiko YAMAMOTO,^a Mizuho AOKI,^b Yoshiya FURUSAWA,^b Koichi ANDO,^b Yasuo KUWABARA,^c Kouji MASUDA,^c Shigeki SASAKI,^a and Minoru MAEDA^{*,a}

^a Faculty of Pharmaceutical Sciences, Kyushu University; ^c Faculty of Medicine, Kyushu University; 3-1-1 Maidashi, Higashi-ku, Fukuoka 812-8582, Japan; and ^b Clinical Radiation Biology and International Space Radiation Laboratory, National Institute of Radiological Sciences; 4-9-1 Anagawa, Inage-ku, Chiba 263-8555, Japan.

Received December 3, 2001; accepted January 24, 2002

In order to develop new imaging markers for brain hypoxia, 4-bromo-1-(3-fluoropropyl)-2-nitroimidazole (4-BrFPN) was designed based on molecular orbital calculations, synthesized and labeled with fluorine-18 as a lipophilic nitroimidazole analog with a lower energy LUMO orbital than those for fluoromisonidazole (FMISO) and 1-(3-fluoropropyl)-2-nitroimidazole (FPN). In an *in vitro* radiosensitization study, the sensitizer enhancement ratio for 4-BrFPN was found to be 1.65 at a 1 mM concentration, in comparison to 1.81 for FMISO. The preparation of ¹⁸F-labeled 4-BrFPN (4-Br¹⁸FPN) was achieved by [¹⁸F]fluoride ion displacement reaction of the tosylate precursor, in a reasonable radiochemical yield (33%, not corrected for decay). Metabolites in tumor and muscle extracts from methylcholanthrene-induced fibrosarcoma mice, as well as the tissue distribution of 4-Br¹⁸FPN in normal rats, were studied. The initial uptake into rat brain of 4-Br¹⁸FPN was significantly higher relative to ¹⁸F-labeled FMISO (¹⁸FMISO), followed by a rapid washout from the brain. The tumor uptake of 4-Br¹⁸FPN was somewhat enhanced compared to those obtained with ¹⁸FMISO and ¹⁸F-labeled FPN (¹⁸FPN), but with lower tumor localization than ¹⁸FMISO. Analyses of tumor and muscle extracts showed metabolites remaining base line on the radio-TLC plates, and they were produced to a greater extent in tumor than muscle. The use of two drugs which increase hypoxic cell fraction in tumor, hydralazine or nitro-L-arginine, produced a significant increase in tumor levels of 4-Br¹⁸FPN, suggestive of a hypoxic mechanism of accumulation. The results imply that lowering of the LUMO energy of a molecule alone is not sufficient to improve its biodistribution properties for better imaging of regions of hypoxia.

Key words nitroimidazole; fluorine-18; brain tissue; tumor; biodistribution

2-Nitroimidazole derivatives typified by misonidazole (MISO), originally developed as hypoxic radiosensitizers for radiation therapy, have been shown to be susceptible to reduction trapping in regions of low oxygen tension. Although the mechanism of nitroimidazole binding to hypoxic tissue is still not fully understood, the nitro group is believed to undergo a one-electron reduction in viable cells to produce a radical anion, while in hypoxic cells this intermediate is further reduced to a species which reacts with cellular components and is hereby trapped within the cell. In normoxic conditions reoxidation rapidly takes place, and the compound eventually diffuses out of the cell.^{1–3} This is the why most efforts to develop selective markers for imaging hypoxic tissue have used 2-nitroimidazole derivatives.⁴

¹⁸F-Labeled fluoromisonidazole (¹⁸FMISO) has shown potential in humans as an agent to map hypoxic tissue with positron emission tomography (PET).^{5–8} However, this agent has drawbacks due to its relatively low concentration within hypoxic tissue and the necessity to wait a long time (2–4 h) to achieve acceptable target-background ratios for imaging. The target tissues have mostly been the myocardium or tumors, with less attention centered on the brain. The utility of ¹⁸FMISO as a hypoxic imaging agent for brain studies appears to be limited because of its low blood–brain barrier (BBB) permeability.^{9,10}

We have been interested in the development of new PET markers exhibiting more rapid localization in the hypoxic region in the brain with a greater BBB permeability than ¹⁸FMISO, based on the same principle of metabolic binding

of nitroreduction products. In a previous paper, we reported the synthesis and evaluation of the two lipophilic 2-nitroimidazoles, 1-(3-[¹⁸F]fluoropropyl)-2-nitroimidazole (¹⁸FPN) and 1-(8-[¹⁸F]fluorooctyl)-2-nitroimidazole (¹⁸FON), as brain-targeted hypoxic imaging agents.¹¹ The high lipophilicity of ¹⁸FPN and ¹⁸FON resulted in the increased initial uptake into normal rat brain, relative to ¹⁸FMISO, but both compounds had significantly lower tumor uptake and lower tumor-to-blood ratios than ¹⁸FMISO, suggestive of a poor trapping mechanism within the tumor tissue. One of the primary reasons for these disappointing results appeared to be the lack of a sufficiently high reduction potential (electron affinity) undergoing more rapid bioreduction of the nitro group. Therefore, we have now designed 4-bromo-1-(3-fluoropropyl)-2-nitroimidazole (4-BrFPN), based on the molecular orbital calculations, to improve the electron affinity property of the 2-nitroimidazole ring, with sufficient lipophilicity to penetrate the BBB to image cerebral hypoxia. In this paper we describe the design, synthesis and radiolabeling with fluorine-18 of 4-BrFPN. Additionally, the *in vivo* biodistribution of this designed compound is also characterized in normal rats and in tumor-bearing mice to evaluate its potential use as a marker of hypoxic tissue in comparison with ¹⁸FMISO and ¹⁸FPN.

RESULTS AND DISCUSSION

Design Reduction potential, as well as lipophilicity, is considered important in the rational design of hypoxia-selective

* To whom correspondence should be addressed. e-mail: maeda@phar.kyushu-u.ac.jp

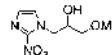
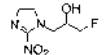
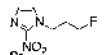
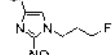
tive nitroimidazoles.¹¹) To predict electron affinity as a measure of the ease of electron gain of a compound, we calculated the orbital energies of the lowest unoccupied molecular orbital (LUMO), with MOPAC98-PM3, for nitroimidazole analogs with additional substituents on the nitroimidazole ring and containing a fluoropropyl group on imidazole nitrogen to maintain lipophilic character for brain targeting. We hypothesized that the decrease of E_{LUMO} of a molecule would result in increased capacity to facilitate metabolic reduction and trapping under hypoxia. The molecular orbital calculations show that the introduction of a bromine atom at the 4-position in the nitro-bearing ring results in a significant lowering of E_{LUMO} , when compared with FPN, FMISO and MISO, as shown in Table 1. Moreover, 4-BrFPN shows the distribution of LUMO on the 2-nitroimidazole ring. Therefore, 4-BrFPN was chosen as a radiosynthetic target of this work to investigate whether the increased electron affinity would lead to improved biodistribution property and/or enhanced hypoxic selectivity.

Synthesis and Lipophilicity Chart 1 shows a synthetic approach to the required 4-BrFPN. The tosylate (**1**) was prepared by coupling di-tosyl propylate with 2-nitroimidazole in the presence of triethylamine in *N,N*-dimethylformamide (DMF), as reported previously.¹¹) Direct bromination of the tosylate (**1**) with an excess amount of Br_2 in dioxane resulted in the formation of the 4-bromo tosylate (**2**). $^1\text{H-NMR}$ and mass spectra of the predicted isolated product indicated that one bromine was substituted on the imidazole ring, but not a mixture of the positional isomers. The preparation of 4-BrFPN (**3**) was accomplished by fluoride substitution on the tosylate precursor (**2**) using tetrabutylammonium fluoride at room temperature in 71% yield. The regioisomeric identification of the 4-bromo isomer was based on the comparison of chemical shifts of $^{13}\text{C-NMR}$ spectra of 4-BrFPN (**3**) and FPN.

The $\log P$ value for 4-BrFPN was measured as an index of lipophilicity by octanol/water extraction at pH 7.4, and is given in Table 1, in which comparison of the $\log P$ values for FMISO, FPN and MISO are also included. 4-BrFPN has a higher partition coefficient than FMISO, FPN and MISO. Thus, the bromine atom on the imidazole ring, borne by 4-BrFPN, has made the compound more lipophilic, but this falls well within the range ($\log P=2.0\pm 1.0$) of lipophilicity thought to be compatible with good BBB penetration by diffusion.

Radiosensitization Hypoxic cell radiosensitizers are generally compounds with high electron affinity, and a correlation between electron affinities (one-electron reduction potentials) and radiosensitizing effectiveness with hypoxic cells has been reported to exist among nitroimidazoles, including MISO.^{12–15}) The radiosensitizing effect of 4-BrFPN on hypoxic Chinese hamster V79 cells was thus investigated, comparing it with those of FMISO and FPN. Since 4-BrFPN has low solubility in H_2O , all *in vitro* radiosensitization experiments were carried out in minimal essential medium (MEM) containing 1% dimethylsulfoxide (DMSO). The profiles of the dose–survival curves of V79 cells observed after X-ray irradiation with 4-BrFPN are shown in Fig. 1. The SER (sensitizer enhancement ratio) for 4-BrFPN was found to be 1.65 at a 1 mM concentration, in comparison to 1.81 for FPN and 1.60 for FMISO (Table 1), indicating that there was no sig-

Table 1. Partition Coefficients, Radiosensitizing Activity, and the Orbital Energy of the LUMO of 2-Nitroimidazole Derivatives

Compound	$\log P$ (octanol/water) ^{a)}	SER ^{d)} (1 mM)	E_{LUMO} ^{e)} (eV)
 MISO	−0.39 ^{b)}	1.44 ^{b)}	−0.79
 FMISO	−0.40 ^{c)}	1.60	−0.96
 FPN	0.28 ^{c)}	1.81 ^{c)}	−1.02
 4-BrFPN	1.09	1.65	−1.18

a) An octanol/water partition coefficient was determined by shaking solutions of compounds in 2.5 ml 1-octanol with 2.5 ml potassium phosphate buffer (pH 7.4) for 20 min, and the data are the average of three separate experiments. b) Calculated from reported p values, ref. 19. c) Values were from ref. 11. d) SER was calculated from the ratio of radiation doses for 10% survival with and without compound, by reading the curve in Fig. 1 for each sensitizer. e) The energy of the lowest unoccupied molecular orbital (E_{LUMO}).

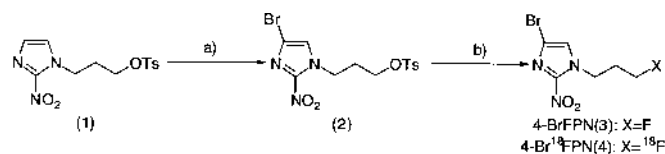


Chart 1

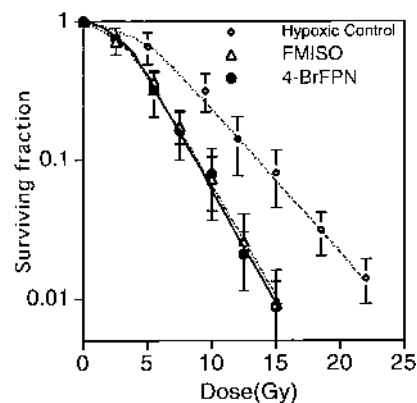


Fig. 1. Radiation Survival Curves of Hypoxic V79 Cells

Cells were incubated with 1 mM concentration of 4-BrFPN (●) or FMISO (Δ) immediately before X-ray irradiation under hypoxic conditions at room temperature, respectively. Each point represents the mean \pm S.E. for 3 experiments. Hypoxic control (◇).

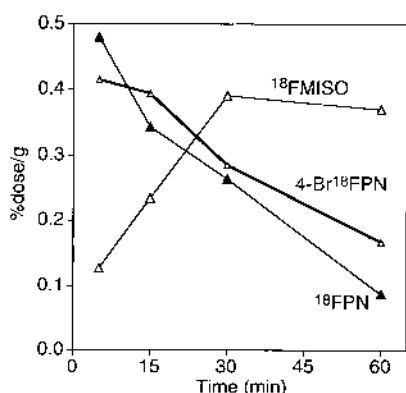
nificant difference in *in vitro* radiosensitizing potentials for the three nitroimidazoles.

Radiosynthesis Radiochemical synthesis was achieved by nucleophilic displacement of a tosylate precursor with a ^{18}F fluoride ion. The no-carrier-added ^{18}F fluoride activity obtained from the $^{18}\text{O}(p,n)^{18}\text{F}$ reaction was converted to K^{18}F /Kryptofix 2.2.2., as described earlier.¹⁶) We found that optimal reaction conditions were a 15 min reaction time at 80 °C in acetonitrile, using the tosylate (**2**) and a Kryptofix 2.2.2.-potassium ^{18}F fluoride complex. The overall synthetic time, including HPLC purification, was 40 min. The isolated radiochemical yield of 4-Br ^{18}F FPN at the end of synthesis was 33% with more than 96% radiochemical purity. The specific

Table 2. Biodistribution of Radioactivity after 4-Br¹⁸FNP Injection in Normal Wistar Rats (*n*=3)

Tissue	Uptake (%dose/g)			
	5 min	15 min	30 min	60 min
Blood	0.353±0.108	0.403±0.060	0.308±0.021	0.228±0.023
Liver	0.811±0.578	1.705±0.213	1.263±0.302	1.471±0.158
Adrenals	0.746±0.398	0.929±0.100	0.649±0.148	0.474±0.030
Kidneys	0.762±0.339	1.385±0.298	0.896±0.196	0.956±0.099
Heart	0.401±0.157	0.481±0.054	0.379±0.040	0.262±0.025
Bone	0.076±0.050	0.133±0.017	0.145±0.040	0.315±0.034
Brain	0.415±0.152	0.394±0.019	0.285±0.031	0.166±0.021

Means±S.D.

Fig. 2. Rat Brain Uptake of Three ¹⁸F-Fluorinated Nitroimidazoles at Different Times after i.v. Injection

Data are the average from three animals. Values for ¹⁸FMISO and ¹⁸FNP were from our previous report: ref. 11.

activity was estimated to be around 3700 GBq/mmol at the end of the synthesis.

In Vivo Biodistribution As shown in Table 2, tissue distribution of 4-Br¹⁸FNP was determined in normal Wistar rats at 5, 15, 30 and 60 min following intravenous injection. At 5 min after injection, the blood concentration was already at low levels, showing fast transport of the tracer to tissue. The extent of defluorination for 4-Br¹⁸FNP, indicated by bone radioactivity, was kept at a low level until 30 min, then slightly increased at 60 min postinjection.

A biological characteristic of 4-Br¹⁸FNP is that both the liver and kidneys showed higher uptake than most other normal tissues, as observed with ¹⁸FMISO and ¹⁸FNP,^{17,18} indicative of extensive metabolism in the liver and urinary excretion. Brain uptake as a function of time after injection is depicted graphically in Fig. 2 with data of ¹⁸FMISO and ¹⁸FNP, which were previously reported. The initial brain radioactivity of 4-Br¹⁸FNP was almost similar to ¹⁸FNP, but significantly higher than ¹⁸FMISO, indicating rapid brain penetration, and its maximal brain uptake occurred at less than 5 min post injection. It should be noted that rapid washout of radioactivity from the brain was observed with no indication of accumulation. Such an uptake and washout pattern of radioactivity observed in the normal brain thus appeared to be a desirable characteristic for a potential agent for imaging hypoxic tissue in the brain.

The biodistribution of 4-Br¹⁸FNP at 30 and 60 min post in-

Table 3. Biodistribution of 4-Br¹⁸FNP in Fibrosarcoma-Bearing C3H Mice

Tissue	Uptake (%dose/g) ^{a)}	
	30 min (<i>n</i> =4)	60 min (<i>n</i> =3)
Blood	3.115±0.157	1.822±0.195
Lund	7.483±1.200	6.722±0.432
Liver	13.429±1.737	11.464±1.168
S. Intestine	10.436±1.141	4.211±1.835
Adrenals	5.607±0.975	3.531±1.024
Kidneys	8.000±0.940	4.154±0.226
Heart	2.881±0.318	1.527±0.025
Tumor	2.423±0.230*	2.152±0.258*
Muscle	1.728±0.237	1.048±0.094
Bone	6.131±1.642	9.226±2.003
Brain	1.585±0.255	0.822±0.025
Tumor/blood	0.777±0.053	1.194±0.214
Tumor/muscle	1.410±0.121	2.050±0.070

a) Mean±S.D. *t*-test: **p*<0.01 compared to muscle data.

jection, in C3H mice bearing transplanted tumors (methylcholanthrene induced fibrosarcoma) as rodent tumor models, was further investigated to assess the accumulation of the tracers in tumor (Table 3). It is generally known that tumors provide a strong reducing environment when compared to normal tissue, and many solid tumors contain hypoxic areas.^{1,19} The tumor cells were implanted in the right leg muscle of C3H mouse and allowed to grow for 9–10 d.

Tumor load did not significantly influence the uptake of 4-Br¹⁸FNP in normal organs, and the tumors showed significant retention of the radioactivity. The concentration of radioactivity in the tumor was 2.4% dose/g at 30 min and 2.1% dose/g at 60 min, which are actually higher than those obtained with ¹⁸FNP (1.5% dose/g at 30 min and 1.6% dose/g at 60 min)¹¹ in the same tumor model. The tumor-to-muscle and tumor-to-blood ratios showed an increase with time: the uptake ratios of the time-to-blood and tumor-to-muscle were 1.19 and 2.05 with 4-Br¹⁸FNP at 60 min postinjection, although with insufficient selectivity, which are significantly high ratios compared with those obtained with ¹⁸F-FNP (0.79 and 1.38).¹¹ Blood samples, obtained from the heart of mice at 60 min after injection of 4-Br¹⁸FNP were examined to determine the distribution of radioactivity in the plasma and red blood cells. We found 75% of the activity in the plasma, of which 74% was distributed in the protein-free plasma fraction, with no radioactivity remaining as the intact parent compound, as shown by radio-TLC analysis (data not shown).

We evaluated the selectivity of 4-Br¹⁸FNP for hypoxic tissues using two pharmacological modulators, hydralazine and nitro-L-arginine, which have been shown to increase the hypoxic cell fraction in tumors.^{20,21} The modulators were injected 40 min before tracer administration, and the mice were killed at 30 and 60 min after injection of 4-Br¹⁸FNP. As shown in Fig. 3, nitro-L-arginine-treated animals showed significantly higher uptake of 4-Br¹⁸FNP, by 40% at 30 min postinjection, compared with the control animals, indicating that the accumulated radioactivity of 4-Br¹⁸FNP in the tumor was at least related to tumor oxygenation. The difference in the experiments with hydralazine did not reach statistical significance regarding tumor uptake.

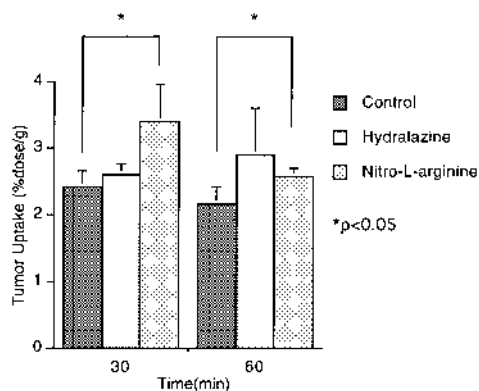


Fig. 3. Uptake of Radioactivity in Mice Fibrosarcoma at 30 and 60 min Postinjection of 4-Br¹⁸FNP, after Injection of Hydralazine or Nitro-L-arginine as a Pharmacological Modulator of Tumor Hypoxia ($n=4$)

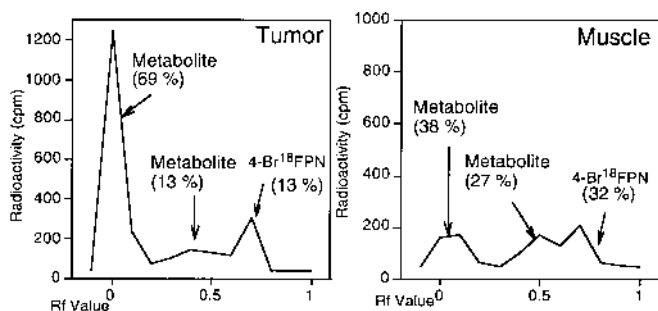


Fig. 4. Radio-TLC Chromatograms of Mouse Tumor and Muscle Extracts at 60 min Postinjection of 4-Br¹⁸FNP

In Vivo Metabolic Study Accumulated radioactivity in the tumor and muscle of mice at 60 min post injection of 4-Br¹⁸FNP were evaluated by radio-TLC for the presence of metabolites. Both tumor and muscle tissues were homogenized in MeOH and then centrifuged. The pellet was then resuspended in MeOH and again centrifuged. The combined supernatant was evaporated, the residue was dissolved with MeOH, and they were passed through Amberlite IRA-410 for the removal of free [¹⁸F]fluoride ion, because the [¹⁸F]fluoride ion and other polar metabolites were not differentiable on radio-TLC. Both samples were analyzed for metabolites by radio-TLC using CHCl₃-MeOH. The extraction of radioactivity from the tumor and muscle was approximately 60%, respectively.

Radio-TLC analysis revealed a major radioactive peak remaining at the origin, indicative of the formation of polar metabolites, in addition to a radioactive species (R_f 0.7) comigrated with authentic 4-BrFNP and a radioactive species with an R_f value of 0.4–0.1 in both extract samples (Fig. 4). Additional TLC analysis showed the absence of a debrominated metabolite, *i.e.*, ¹⁸FNP, which was presumed to be produced as one of the metabolites. Radioactivity remaining at the origin of the TLC plate accounted for 69% in tumor extracts, whereas that in muscle extracts comprised 38%. Based on the solvent extraction procedure used here, free [¹⁸F]fluoride ion did not contribute significantly to the origin radioactivity on TLC. Thus, metabolites remaining base line on the TLC plates, which were found to a greater extent in tumor than muscle, may reflect bioreductive metabolism and binding within the tumor hypoxic tissue, although further experi-

mentation is necessary. Differential distribution of radioactivity on the radio-TLC between tumor and muscle extracts, closely similar to that found with 4-Br¹⁸FNP, was also observed with ¹⁸FMISO (data not shown).

CONCLUSION

With the aim of developing a new hypoxia-imaging agent in the brain, we have designed (from a simple frontier molecular orbital standpoint), synthesized and evaluated a new 2-nitroimidazole analog bearing a bromine atom on the imidazole ring, 4-Br¹⁸FNP. 4-Br¹⁸FNP offered enhanced tumor-to-blood and tumor-to-muscle ratios compared with non-brominated analogs ¹⁸FNP, showing similar radioactivity clearance from the blood and muscle for these two analogs, presumably as a result of favorable changes in the LUMO energy level. A hypoxic mechanism of accumulation is likely to play a role in the tumor uptake of 4-Br¹⁸FNP, as revealed by metabolic analysis and pharmacological modulator studies. However, when compared with ¹⁸FMISO with a higher energy LUMO orbital, 4-Br¹⁸FNP showed lower tumor localization than ¹⁸FMISO, although the tumor-to-background ratios for these two analogs do not differ substantially at 30–60 min post injection. The results provide an implication that lowering of the LUMO energy of a molecule alone is not sufficient to improve biodistribution properties for better imaging of regions of hypoxia. Based on the findings of this study, we are now focusing attention on designing analogs with more selective uptake in hypoxic tissue and less non-reductive metabolism.

MATERIALS AND METHODS

Unless otherwise stated, chemical reagents were obtained from commercial sources and were used directly. All melting points are uncorrected. ¹H-NMR spectra were obtained on a JEOL GX-270 spectrometer (270 MHz), and the chemical shifts are reported in parts per million downfield from tetramethylsilane. ¹³C-NMR spectra were obtained on a Varian Unity 500 spectrometer (125 MHz), and the chemical shifts are reported in parts per million downfield from tetramethylsilane. Infrared (IR) spectra were recorded with a JASCO IR Report-100 spectrometer. Mass spectra were obtained with a JEOL JMS DX-610 or SX-102 mass spectrometer. Column chromatography was performed on Kieselgel 60 (70–230 mesh, Merck), and analytical TLC and radio-TLC was carried out on Silica gel 60F 254 (Merck). In the synthetic procedures, organic extracts were routinely dried over anhydrous Na₂SO₄ and evaporated with a rotary evaporator under reduced pressure. HPLC was done using a TOSOH CCP & 8020 series HPLC system fitted with a Whatman Partisil 5PAC (10×100 mm) with monitoring of the radioactivity as well as UV absorption (at 254 nm). The radioactivity was also quantified with a Capintec radioisotope calibrator (CRC-30). The identity of radiolabeled compounds was supported by HPLC co-injection studies.

Fluorine-18 was produced from 8 or 16% enriched [¹⁸O]H₂O by the ¹⁸O(p,n)¹⁸F reaction, as described previously.²² Aminopolyether (Kryptofix 2.2.2.)-supported potassium [¹⁸F]fluoride (K¹⁸F/Kryptofix) was prepared by the addition of K₂CO₃·1.5H₂O (1.0 mg) and Kryptofix 2.2.2. (3.0 mg) to irradiated water in a TPX (polymethylpentene)

vessel, and by subsequent removal of the water under a stream of argon at 110 °C by azeotropic distillation with dry CH₃CN. Radiochemical yields were expressed at the end-of-synthesis (not corrected for decay), relative to the amount of the [¹⁸F]fluorinating agent measured as total radioactivity present in the reaction vessel. All animal experiments were carried out in accordance with the regulations on animal experiments of the Faculty of Pharmaceutical Sciences, Kyushu University.

4-Bromo-1-*N*-(3-*p*-toluenesulfonyloxypropyl)-2-nitroimidazole (2) Under argon, to a solution of 1-*N*-(3-*p*-toluenesulfonyloxypropyl)-2-nitroimidazole¹¹⁾ (1) (50.7 mg, 0.156 mmol) in dry 1,4-dioxane (2 ml) was added dropwise bromine (100 μl) using a syringe. The mixture was stirred at room temperature for 24 h and evaporated to dryness for the removal of excess bromine. The residue was chromatographed on silica gel (EtOAc:Hexane=1:4) to give 4-bromo-1-*N*-(3-*p*-toluenesulfonyloxypropyl)-2-nitroimidazole (2) (49.7 mg, 79%) as a pale yellow powder, mp 70–75 °C. ¹H-NMR (CDCl₃) δ (ppm): 7.798 (d, 2H, *J*=8.3 Hz, Ar-H), 7.398 (d, 2H, *J*=7.9 Hz, Ar-H), 6.984 (s, 1H, NCB=C_HN), 4.500 (t, 2H, *J*=6.6 Hz, NCH₂CH₂CH₂OTs), 4.054 (t, 2H, *J*=5.6 Hz, NCH₂CH₂CH₂OTs), 2.481 (s, 3H, Ar-CH₃), 2.243 (tt, 2H, *J*=6.9, 5.6 Hz, NCH₂CH₂CH₂OTs). IR (Nujol): 3120, 1740, 1585, 1530 cm⁻¹. FAB-MS *m/z*: 404 (M⁺), 406 (M+2). High resolution (HR)-MS (FAB-MS). Calcd for C₁₃H₁₅BrSN₃O₅: 403.9916 (MH⁺). Found: 403.9944.

4-Bromo-1-*N*-(3-fluoropropyl)-2-nitroimidazole (4-BrFPN) (3) Under argon, to a solution of 4-bromo-1-*N*-(3-*p*-toluenesulfonyloxypropyl)-2-nitroimidazole (2) (49.0 mg, 0.121 mmol) in dry tetrahydrofuran (THF) (1 ml) was added dropwise a 1M-THF solution of *n*-Bu₄NF (0.50 ml, 0.50 mmol as F⁻). The mixture was stirred at room temperature for 6 h and evaporated to dryness. The residue was chromatographed on silica gel (EtOAc:hexane=1:1) to give 4-bromo-1-*N*-(3-fluoropropyl)-2-nitroimidazole (3) (21.9 mg, 71%) as a pale yellow oil. ¹H-NMR (CDCl₃) δ (ppm): 7.171 (s, 1H, NCB=C_HN), 4.592 (t, 2H, *J*=6.9 Hz, NCH₂CH₂CH₂F), 4.517 (dt, 2H, *J*=46.9, 5.5 Hz, NCH₂CH₂CH₂F), 2.284 (dt, 2H, *J*=27.1, 6.9, 5.5 Hz, NCH₂CH₂CH₂F). ¹³C-NMR (CDCl₃) δ (ppm): 125.9 (s, 5-C), 115.3 (s, 4-C), 79.9 (d, *J*=167.0 Hz, NCH₂CH₂CH₂F), 47.03 (s, 2-C), 47.00 (s, NCH₂CH₂CH₂F), 30.8 (d, *J*=19.4 Hz, NCH₂CH₂CH₂F). IR (Nujol): 3125, 2960, 1530, 1500, 1465, 1365 cm⁻¹. FAB-MS *m/z*: 252 (M⁺), 254 (M+2). HR-MS (FAB-MS). Calcd for C₆H₈BrFN₃O₂: 251.9784 (MH⁺). Found: 251.9769.

4-Bromo-1-*N*-(3-[¹⁸F]fluoropropyl)-2-nitroimidazole (4-Br¹⁸FPN) (4) 4-Bromo-1-*N*-(3-*p*-toluenesulfonyloxypropyl)-2-nitroimidazole (2) (1 mg, 2.47 mmol) dissolved in dry CH₃CN (300 μl) was added to a TPX vessel containing the K¹⁸F/Kryptofix 222 (136.5 MBq). The vessel was closed and heated in an oil bath at 80 °C for 15 min, then cooled to room temperature. The reaction mixture was filtered through Sep-Pak Silica with EtOAc (3 ml). The filtrate was evaporated *in vacuo*. The residue was dissolved in hexane:EtOAc=3:1 (1 ml) and injected into the HPLC (Whatman Partisil 5PAC, 10×100 mm, hexane:EtOAc=3:1, 2 ml/min). The radioactive fraction eluted at *t*_R=5.5 min, corresponding to authentic 4-BrFPN, was collected. Total synthetic time was 40 min. The radiochemical yield (not corrected for decay) was 33%. No radiochemical impurities were detected by HPLC.

Partition Coefficients The log *P* value was measured using a standard shake flask method. The sample was shaken well with a mixture of 1-octanol (2.5 ml) and 0.05 M phosphate buffer (2.5 ml, pH 7.4) for 20 min at 25 °C, after which aliquots of both phases were taken for analysis by HPLC quantitation. The reported log *P* value represents the mean of three experiments.

Radiosensitization Radiosensitization studies were carried out by employing Chinese hamster V79 cells, and the radiation used was 200 kVp X-rays. All experiments were carried out in glass culture dishes, gassed at room temperature with humidified nitrogen or air for oxic controls. Just before X-irradiation, the culture medium was exchanged to a fresh medium, including 1% DMSO and 1 mM concentration of 4-BrFPN or FMISO. The cells were irradiated at room temperature under hypoxic conditions. Cell survival was determined using a conventional colony-forming assay. After post irradiation treatment, the test compound was removed by two washings with PBS buffer solution. Subsequently, cells that were trypsinized and suspended in fresh medium were counted, diluted, and plated on culture dishes. After incubation for 6 d, the colonies were then fixed with 10% formalin PBS buffer solution, stained with 1% methylene blue, and then counted; survival curves were then constructed. All experiments were performed at least in triplicate. Radiosensitization was measured as the mean of the SER calculated at a 10% survival level.

Biodistribution in Normal Rats Male Wistar rats (7 weeks old, 215–240 g) given standard laboratory food and water *ad libitum* were used in this investigation. Aliquots of 4-Br¹⁸FPN in about 200 μl of saline solution, with activities ranging from 1.75–2.98 MBq, were injected through the tail vein of unanesthetized rats. After the given time intervals, the animals were killed by cervical dislocation while under ether anesthesia. All samples of either the blood or the organ of interest that had been blotted free of blood, were taken and weighed. The radioactivity of all samples was measured with an Aloka AutoWell Gamma System ARC-400 (corrected for decay), and the percent injected dose per gram of tissue weight (%dose/g) was then calculated for each type of tissue.

Biodistribution in Tumor-Bearing Mice 3-Methylcholanthrene-induced fibrosarcoma (NFSa) was inoculated *s.c.* into the right hind leg muscle of female C3H/He mice (5 weeks old, 18.0–21.0 g). Tumors which developed with a diameter of about 1 cm at 9–10 d after inoculation were used.¹¹⁾ The animals were allowed free access to water and food at all times. Aliquots of 4-Br¹⁸FPN in about 200–300 μl of saline solution, with activities ranging from 0.47–2.83 MBq, were injected through the tail vein of unanesthetized mice. At 30 and 60 min post injection, the animals were killed by cervical dislocation while under ether anesthesia. Samples of blood and the tissues of interest, blotted free of blood, were taken, weighed, and assayed for radioactivity in an Aloka Auto Well Gamma System ARC-400 (corrected for decay). The results are expressed as the percent injected dose per gram (%dose/g) of tissue weight, and tumor-to-blood and tumor-to-muscle concentration ratios were calculated from the %dose/g tissue data.

Blood samples obtained from the heart at 60 min post injection of 4-Br¹⁸FPN were placed in heparinized vials, then centrifuged (2000 rpm, 10 min), and the plasma was re-

moved. The red blood cells (RBC) were washed with a small amount of ice-cold saline and the wash was added to the plasma. Aliquots of the plasma solution and the total RBC pellet were counted for ^{18}F activity. An equal volume of freshly prepared 1 M HClO_4 (PCA) was added to the plasma, and the combined mixture was centrifuged (2000 rpm, 5 min) to remove precipitated proteins. The supernatant and one PCA washing were combined. The plasma protein and the protein free-plasma were also counted for ^{18}F activity. Aliquots of protein free-plasma were spotted on TLC plates, then developed with hexane:EtOAc=1:1. The TLC plate content was counted with a radio-TLC analyzer. The location of 4-Br ^{18}F FPN on the plate was determined by co-spotting with an authentic cold sample.

Pharmacological modulator studies were performed using hydralazine and nitro-L-arginine. Hydralazine (5 mg/kg, i.p.) or nitro-L-arginine (10 mg/kg, i.v.) was injected at 40 min before tracer administration. Thirty and sixty minutes after 4-Br ^{18}F FPN injection, the mice were killed and the tumor and muscle were prepared and counted as described above.

In Vivo Metabolic Study Aliquots of 4-Br ^{18}F FPN in 200 μl of saline solution, with activities ranging from 2.19—13.3 MBq, were injected through the tail vein of unanesthetized fibrosarcoma-bearing mice (17.6—19.5 g). At 60 min postinjection, the animals were killed by cervical dislocation while under ether anesthesia. Tumor and muscle tissue was taken, homogenized and extracted with methanol under an ice-cooled condition, respectively. The respective extract solution was centrifuged (3000 rpm \times 10 min), and the supernatant was concentrated *in vacuo* and filtered through Amberlite IRA-410 (Cl^- form, 30 mg) to remove free [^{18}F]fluoride. A control experiment using the resin was performed with authentic [^{18}F]fluoride ion to determine the removal capability of [^{18}F]fluoride ion, and to validate the procedure. Aliquots of the filtered solution were spotted on TLC plates, then developed with chloroform:methanol=4:1. The TLC plates were cut into 0.5 mm wide strips, and their radioactivities were counted with an Aloka Auto Well Gamma System ARC-400. The location of 4-Br ^{18}F FPN and ^{18}F FPN on the plates was determined by co-spotting with the authentic sample, respectively.

Statistical Analysis All values of radioactivity in animals were expressed as the mean \pm S.D. Lack of significance using Student's *t*-test was considered to be $p>0.05$.

Acknowledgments We are indebted to the staff of the

Kyushu University Medical School Cyclotron Facility for their assistance in producing ^{18}F . The support of this work by a Grant-in-Aid for Scientific Research from the Ministry of Education, Science, Sports and Culture of Japan is gratefully acknowledged.

REFERENCES

- 1) Chapman J. D., *N. Engl. J. Med.*, **301**, 1429—1432 (1979).
- 2) Franko A. J., Koch C. J., Garrecht B. M., Sharplin J., Hughes D., *Cancer Res.*, **47**, 5367—5376 (1987).
- 3) Edwards D. I., *J. Antimicrob. Chemother.*, **31**, 9—20 (1993).
- 4) Nunn A., Linder K., Strauss H. W., *Eur. J. Nucl. Med.*, **22**, 265—280 (1995).
- 5) Casciari J. J., Rasey J. S., *Radiat. Res.*, **141**, 28—36 (1995).
- 6) Jerabek P. A., Patrick T. B., Kilbourn M. R., Dischino D. D., Welch M. J., *Appl. Radiat. Isot.*, **37**, 599—605 (1986).
- 7) Prekeges J. L., Rasey J. S., Grunbaum Z., Kenneth H., *Biochem. Pharmacol.*, **42**, 2387—2395 (1991).
- 8) Martin G. V., Cerqueira M. D., Caldwell J. H., Rasey J. S., Embree L., Krohn K. A., *Circ. Res.*, **67**, 240—244 (1990).
- 9) Mathias C. J., Welch M. J., Kilbourn M. R., Jerabek P. A., Patrick T. B., Raichle M. E., Krohn K. A., Rasey J. S., Shaw D. W., *Life Sci.*, **41**, 199—206 (1987).
- 10) Liu R. S., Yeh S. H., Guo W. Y., Pan D. H. C., Lee L. S., Chu L. S., Chang C. P., Wang J. K., Wu L. C., *J. Nucl. Med.*, **36**, 53P (1995).
- 11) Yamamoto F., Oka H., Antoku S., Ichiya Y., Masuda K., Maeda M., *Biol. Pharm. Bull.*, **22**, 590—597 (1999).
- 12) Adams C. E., Clarke E. D., Flockhart I. R., Jacobs R. S., Sehmi D. S., Stratford I. J., Wardman P., Watts M. E., Parrick J., Wallace R. G., Smithen C. E., *Int. J. Radiat. Biol.*, **35**, 133—150 (1979).
- 13) Adams C. E., Clarke E. D., Gray P., Jacobs R. S., Stratford I. J., Wardman P., Watts M. E., Parrick J., Wallace R. G., Smithen C. E., *Int. J. Radiat. Biol.*, **35**, 151—160 (1979).
- 14) Adams C. E., Flockhart I. R., Smithen C. E., Stratford I. J., Wardman P., Watts M. E., *Radiat. Res.*, **67**, 9—20 (1976).
- 15) Workmann P., Brown J. M., *Cancer Chemother. Pharmacol.*, **6**, 39—49 (1981).
- 16) Yamamoto F., Sasaki S., Maeda M., *Appl. Radiat. Isot.*, **43**, 633—639 (1992).
- 17) Hoffman J. M., Rasey J. S., Spance A. M., Shaw D. W., Lrohn K. A., *Stroke*, **18**, 168—176 (1987).
- 18) Van Os-Corby D. J., Chapman J. D., *Int. J. Radiat. Oncol. Biol. Phys.*, **12**, 1251—1254 (1986).
- 19) Grunbaum Z., Freauff S. J., Krohn K. A., Wilbur D. S., Magee S., Rasey J. S., *J. Nucl. Med.*, **28**, 68—75 (1987).
- 20) Wood P. J., Stratford I. J., Sanson J. M., Cattanach B. M., Quinney R. M., Adams G. E., *Int. J. Radiat. Oncol. Biol. Phys.*, **22**, 473—476 (1992).
- 21) Wood P. J., Stratford I. J., Adams G. E., Szabo C., Thiemermann C., Vane J. R., *Biochem. Biophys. Res. Commun.*, **192**, 505—510 (1993).
- 22) Maeda M., Fukumura T., Kojima M., *Appl. Radiat. Isot.*, **38**, 307—310 (1987).